applied sciences

MDPI

Article

A High Peak Power and High Beam Quality Sub-Nanosecond Nd:YVO_4 Laser System at 1 kHz Repetition Rate without SRS Process

Yutao Huang [1,2,3], Hongbo Zhang [1,2,3], Xiaochao Yan [1,2], Zhijun Kang [1,2], Fuqiang Lian [1,2] and Zhongwei Fan [1,2,3,*]

1 Academy of Opto-Electronics, Chinese Academy of Sciences, Beijing 100094, China; yutaohuang@126.com (Y.H.); hbzhang999@126.com (H.Z.); yanxc123@126.com (X.Y.); kzjun1221@126.com (Z.K.); aoefiberlaser@126.com (F.L.)
2 National Engineering Research Center for DPSSL, Beijing 100094, China
3 University of Chinese Academy of Sciences, Beijing 100049, China
* Correspondence: fanzhongwei@aoe.ac.cn; Tel.: +86-10-8217-8609

Received: 6 November 2019; Accepted: 27 November 2019 ; Published: 2 December 2019

Abstract: We present a compact sub-nanosecond diode-end-pumped Nd:YVO_4 laser system running at 1 kHz. A maximum output energy of 65.4 mJ without significant stimulated Raman scattering (SRS) process was obtained with a pulse duration of 600 ps, corresponding to a pulse peak power of 109 MW. Laser pulses from this system had good beam quality, where $M^2 < 1.6$, and the excellent signal to noise ratio was more than 42 dB. By frequency doubling with an LBO crystal, 532 nm green light with an average power of 40.5 W and a power stability of 0.28% was achieved. The diode-end-pumped pump power limitation on a high peak power amplifier caused by the SRS process and thermal fracture in bulk Nd:YVO_4 crystal is also analyzed.

Keywords: sub-nanosecond laser; high peak power; Nd:YVO_4; stimulated Raman scattering (SRS); thermal fracture

1. Introduction

Compact diode-pumped solid state lasers with high-energy sub-nanosecond pulses at kHz repetition rates have a variety of applications, such as laser ranging [1,2], materials processing [3], nonlinear optical conversion [4,5] and Mid-IR optical parametric processes [6–10], etc.

The scaling of energy from sub-nanosecond oscillators is strongly limited by optical damage and thermal effect. Laser radiation with high beam quality, short pulse duration, high repetition rate, and high intensity can be obtained with the Master Oscillator Power Amplifier (MOPA) approach [11,12]. Both Yb^{3+}-doped lasers [13] and Nd^{3+}-doped lasers [14] can use the MOPA approach to achieve high energy sub-nanosecond pulses near 1 μm. Yb^{3+}-doped lasers have wide gain bandwidth, high Stokes efficiency, and high saturation fluence and achieve pulse energy with hundreds of mJ. In Yb^{3+}-doped lasers, cryogenic cooling is needed to acquire a four-level system, which will increase complexity of laser system [15,16]. Nd^{3+}-doped lasers with four-level systems operating in room temperature have higher gain and simpler structure, making them more attractive.

Several diode-pumped solid-state sub-nanosecond laser systems with different Nd^{3+}-doped materials geometry have been reported recently. A Nd^{3+}-doped amplifier in bounce geometry has higher small-signal gain to amplify sub-nanosecond oscillator with low energy and high repetition. A sub-nanosecond laser using a side-pumped Nd:YVO_4 bounce amplifier operating at 1–10 kHz was demonstrated with 577 ps duration and 545 μJ energy (1 MW peak power) in 2010 [17]. In a 2011 study, a sub-nanosecond Nd:YAG laser system with bounce geometry has been reported, the output

energy of which was 0.8 mJ with peak power of 9.35 MW [18]. However, due to the small volume of the active medium, the pulse energy of a sub-nanosecond laser using bounce geometry is less than 1 mJ. In comparison, Nd^{3+}-doped lasers based on bulk crystal may acquire high pulse energy at the kHz level [19–21]. A sub-nanosecond single frequency MOPA laser system operating at 500 Hz was reported, which generated pulses with a width of 830 ps, energy of 13 mJ, peak power of 15.7 MW, and $M^2 < 1.4$ [22]. A Nd:YAG laser system based on the MOPA approach operating at 300 Hz and using selectable 350–600 ps nominally flat temporal pulse shape has been reported, which generate pulses with 127 mJ energy and maximum peak power of 400 MW [23], but beam quality M^2 were not measured. As is already known, beam quality always gets worse due to thermally induced birefringence in Nd:YAG crystal [21,24]. Laser systems based on end-pumped bulk Nd:YVO_4 crystal have better beam quality because of natural birefringence architecture, which can alleviate thermally induced birefringence [25–27]. At the same time, Nd:YVO_4 is a self-excited Raman scattering crystal [28–30]. Stimulated Raman scattering (SRS) is a third-order nonlinear optical effect, which must be taken into consideration in high peak power amplification. Through the SRS process in YVO_4 crystal, 1064 nm fundamental wave will be converted to Raman light, which consists of different Stokes waves, such as first Stokes wave λ = 1176 nm. Raman light brings in many disadvantages, for example, Raman light consumes amplified fundamental pulse energy and reduces the amplification efficiency. Morever, Raman light with high peak power may enter into the end-pumped laser diode and leads to damage of the laser diode. Because of this, the SRS process should be averted to improve amplification efficiency and keep optical components safety.

In this paper, we present a Sub-Nanosecond Nd:YVO_4 MOPA system consisting of a master and a series of amplifiers. By suppressing the SRS process during amplification, we obtain 65.4 mJ energy at 1064 nm with 600 ps and peak power above 100 MW at 1 kHz. The M^2 is less than 1.6 and the signal to noise ratio can be up to 42 dB. We also analyze the influence of SRS on working parameters in a high peak power Nd:YVO_4 amplifier. After frequency doubling, 40.5 mJ 532 nm green light is achieved with conversion efficiency of 61.8% and one hour power stability of 0.28% (RMS).

2. Experiment Setup

Figure 1 shows the layout of the laser system, which comprises one master oscillator, one four-pass high gain pre-amplifier, and three stages of main amplifier.

The master oscillator is a commercial industrial-grade sub-nanosecond Nd:YVO_4 Q-switched laser (Picolo AOT, InnoLas Laser, Munich, Germany), providing 1064 nm light, with 55 μJ, 450 ps at 1 kHz. Pulses from the Nd:YVO_4 Q-switched laser pass through an optical isolator composed of a PBS, an FR, and a HWP to avoid unwanted reflected light or even optical damage to the master oscillator. Before they are injected into the pre-amplifier, laser pulses are aligned and expanded to 2.0 mm with a beam expander (BE1), which suits the pump mode of the pre-amplifier. The pre-amplifier is an off-axis four-pass diode-end-pumped Nd:YVO_4 amplifier, where the Nd:YVO_4 crystal is $4 \times 4 \times 10$ mm^3, a-cut, 0.3%-doped, and has double-end-wedged cut at 2°. Both sides of the Nd:YVO_4 have been coated to transmission of 1064 nm and 808 nm. The crystal is end-pumped by a 500 W quasi-CW (QCW) fiber-coupled diode (E15F8S22-808.3-500Q-IS39, DILAS, Mainz, Germany), with pump cycle 100 μs at 808 nm. Light from the pump diode is coupled into an 800 μm core fiber, the output of which is focused into Nd:YVO_4 crystal with a spot diameter of 2.4 mm. A plane–concave lens (Lens1) is used for compensating thermal lens of Nd:YVO_4. To achieve compact architecture, a prism is used to reflect light and decrease off-axis angle to keep uniformity of amplified beam. A TFP, an FR, and a HWP are used as an isolator to output amplified pulses.

The pulses are further amplified in a main amplifier which composes of three stages, as illustrated in Figure 1. The main amplifier with single-pass form has high optical efficiency. In consideration of suppression of SRS effect and thermal fracture in gain medium, each amplifier stage has two identical sub-amplifiers. The gain medium in the main amplifier is 0.2 at.% doped Nd:YVO_4 crystals with the same length of 15 mm and double-end-wedged cut at 2°, but have different apertures: crystals at stage 1

are 5 × 5 mm^2, crystals at stage 2 are 6 × 6 mm^2, and crystals at stage 3 are 7 × 7 mm^2. Both sides of the Nd:YVO_4 have been coated to transmission of 1064 nm and 808 nm. Each sub-amplifier was pumped by 50 mJ, 100 µs (10% duty cycle) pulses provided by a 500W QCW fiber coupled diode (E15F8S22-808.3-500Q-IS39, DILAS, Mainz, Germany) operating at 808 nm. Coupling ratios of the pump beam at each amplifier stage are 1:3.7/1:5/1:5.5. Beam expanders (BE2–BE4) are used to mode matching of different stages for good beam quality. Focal length of plane–concave lens (Lens2–Lens4) used for compensating thermal lens of every stage's Nd:YVO_4 crystals are 500 mm, 800 mm, and 1000 mm respectively. A 9 × 9 × 20 mm^3 type I LBO (θ = 90°, ϕ = 10.8°) crystal is used for the extra-cavity frequency doubling.

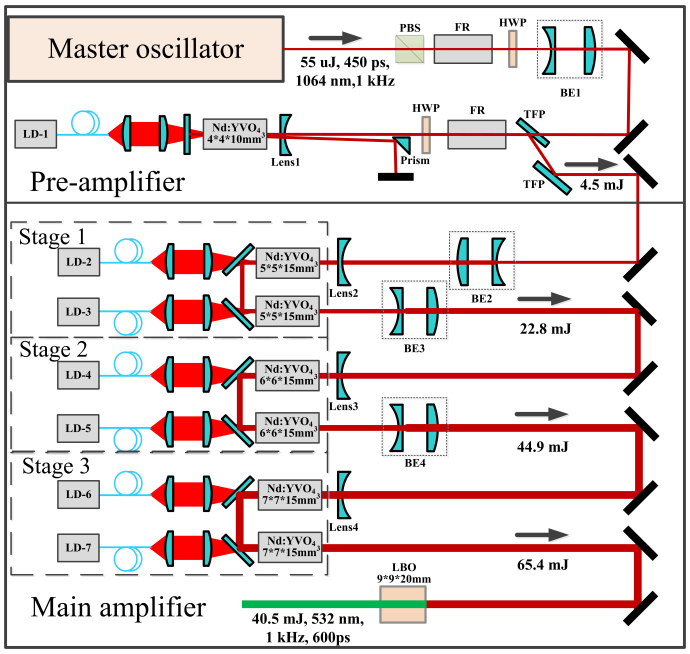

Figure 1. Schematic of the laser system. PBS: polarization beam splitter; FR: Faraday rotator; HWP: half-wave plate; BE: beam expander; TFP: thin-film plate; LD: laser diode.

3. Experimental Results and Discussions

3.1. Pre-Amplifier

A regenerative amplifier has also been used as the pre-amplifier. The regenerative amplifier with Nd:YAG as gain medium could suppress the ASE effect through loss of control by the pockels cell, and achieved higher energy of about 10 mJ. However, the time signal to noise ratio after regenerative amplifier was only 23 dB due to leakage pre-pulses from the pockels cell. The time signal to noise ratio after further amplification decreased to only 10 dB, and the pre-pulse energy was amplified to 7.7 mJ, which could consume energy stored in gain medium, as shown in Figure 2. A pulse picker after regenerative amplification based on electro-optic switches can eliminate pre-pulses and improve the time signal to noise ratio to 40 dB [25], but this will increase system complexity. In order to improve time signal to noise ratio and decrease system complexity, we designed an off-axis four-pass diode-end-pumped Nd:YVO_4 amplification architecture as the pre-amplifier, which could provide high gain with excellent time signal to noise ratio. With an input energy of 55 µJ and 28.6 mJ pump energy into the pre-amplifier stage, up to 4.5 mJ pulse energy at 1 kHz was acheived, and the gain of the pre-amplifier stage could reach 81. With further amplification, the time signal to noise ratio after main amplification was still excellent, which was measured by a photodetector (DET10A, Thorlabs), as shown in Figure 3. To increase the dynamic range of the time signal to noise ratio, the photodetector was overexposed to get the pre-pulse amplitude (2 mV), as shown in Figure 3a. Then the main pulse

was reduced to 1/100 with a filter. The amplitude of the main pulse was 385 mV within the linear range of the photodetector. The time signal to noise ratio was better than 42 dB.

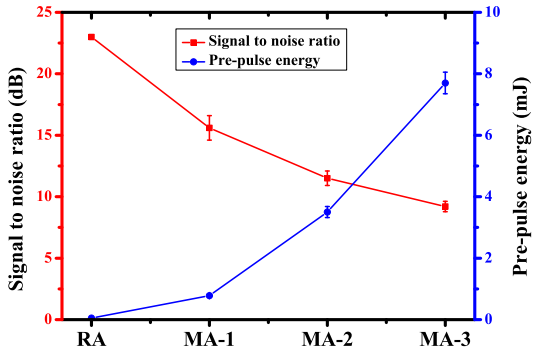

Figure 2. Signal to noise ratio and pre-pulse energy at different amplifiers when a regenerative amplifier was used as the pre-amplifier.

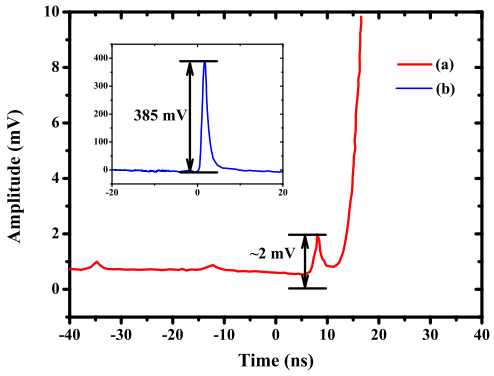

Figure 3. Time signal to noise ratio of maximum output energy: (**a**) Pre-pulse amplitude when the photodetector was overexposed; (**b**) main pulse amplitude when the photodetector was operated in the linear range.

3.2. Main Amplifier and Suppression of SRS effect

In the Nd:YVO_4 crystal of the main amplifier, the maximum peak power of the amplified pulse can reach about 100 MW, which can easily bring about stimulated Raman scattering (SRS). In the progress of SRS, the Stokes wave of Raman light has power gain $exp(G)$. The exponent G is given by

$$G = g_R IL \tag{1}$$

where g_R is the Raman gain, I is the amplified fundamental pulse intensity, and L is the length of the nonlinear Raman medium. The first Stokes wavelength beams will appear when G is 25–30 [31]. The Raman gain of g_R of YVO_4 crystal is 16.13 cm/GW [32]. So when

$$IL \leq 1.55 \text{ GW/cm} \tag{2}$$

the Raman gain in YVO_4 crystal will be below the threshold of SRS progress, and YVO_4 crystal cannot produce the Stokes wave. In our experiment, a 1064 nm laser with intensity of 2.65 GW/cm^2 was once injected into a Nd:YVO_4 crystal with a length of 1.5 cm, which brought about the first Stokes wave (λ = 1175.84 nm), as shown in Figure 4. The Raman shift of Nd:YVO_4 was 890 cm^{-1}, which was almost the same as that of YVO_4 crystal. After passing through Nd:YVO_4 crystal, the energy loss of fundamental 1064 nm laser reached to 20%. Therefore, the generation and accumulation of Raman

light must be prevented in pulse amplification. However, this will affect the working parameters of the Nd:YVO_4 amplifier.

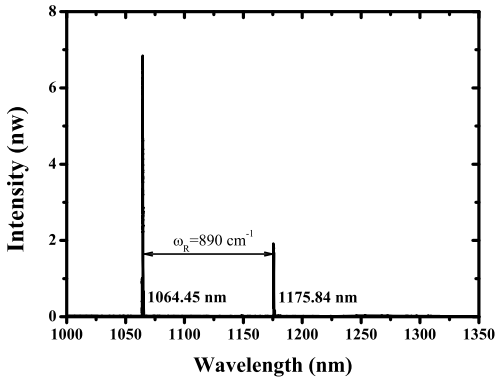

Figure 4. Obtained spectrum of first Stokes wave of Raman light as high intensity laser passing through the Nd:YVO_4 crystal.

The laser intensity continues to increase as the amplification based on the Nd:YVO_4 amplifier increases. To avoid the SRS process, Equation (2) must be satisfied in a high peak power amplifier.

$$\int_0^L I(l)dl \leq 1.55 \text{ GW/cm} \tag{3}$$

What is more, if

$$I_{max}L \leq 1.55 \text{ GW/cm} \tag{4}$$

There will be no significant Raman light. I_{max} is the maximum intensity in the amplification process. So the crystal length L in an amplifier based on Nd:YVO_4 is limited to the maximum amplified intensity for averting the SRS process. At the same time, crystal length L also affects the absorption efficiency of pump light of end-pumped Nd:YVO_4 crystal. To obtain enough absorption efficiency, absorption coefficient α and crystal length L in an end-pumped configuration should satisfy Equation (5) [33].

$$\alpha L = 4 \sim 5 \tag{5}$$

However, absorption coefficient α is an important factor of crystal thermal fracture. According to Reference [33,34], thermal fracture limits pump power for end-pumped Nd:YVO_4 crystal. During the QCW pump operation, the generally accepted way to avoid thermal fracture is pumping the crystal with an average power less than thermal fracture pump power P_{av}, which is less than the fracture pump power P_{cw} of CW pump operation. The maximum pump power at QCW operation is given by

$$P_{av} = \eta P_{cw} = \eta \frac{1}{\alpha} \frac{4\pi R}{\xi} \tag{6}$$

η is the correction factor, which depends on QCW pump duty cycle and repetition, considering a QCW pump duty cycle of 10% in Nd:YVO_4 crystal, $\eta \approx 0.6$ [34]. R is thermal shock parameter depending on the mechanical and thermal properties of the host material. ξ is the fractional thermal loading. When Nd:YVO_4 crystal is pumped with 808 nm, $\frac{4\pi R}{\xi}$ is about 250 W/cm [33]. Based on Equation (6), we can see that thermal fracture pump power P_{av} strongly depends on α. Lowering the dopant concentration can decrease the absorption coefficient and increase the fracture-limited pump power. But in high peak power amplifier, suppression of the SRS process and pump light absorption efficiency also limit the min absorption coefficient. With Equations (4)–(6), to avert the SRS process, when operating the QCW pump, the thermal fracture pump power P_{av} depends on the pulse intensity and can be given by:

$$P_{av} \simeq 100 \frac{\eta}{I_{max}} \tag{7}$$

Figure 5 shows the relationship between the maximum pump power and the maximum laser intensity at QCW pump duty cycle of 10% and 1 kHz level for Nd:YVO_4 amplifier, which is described as Equation (7). It can be seen that, the higher amplified intensity is the lower the maximum pump power will be. When the amplified intensity is 1 GW/cm^2, the maximum pump power approaches 60 W. But when the amplified intensity increases to 4 GW/cm^2, the maximum pump power decreases to 15 W. At high peak power amplifier, the diode-end-pumped power for bulk Nd:YVO_4 is limited to suppression of the SRS process and thermal fracture of bulk Nd:YVO_4 crystal. Therefore, the amplification ability of an end-pumped Nd:YVO_4 amplifier is limited to the laser intensity.

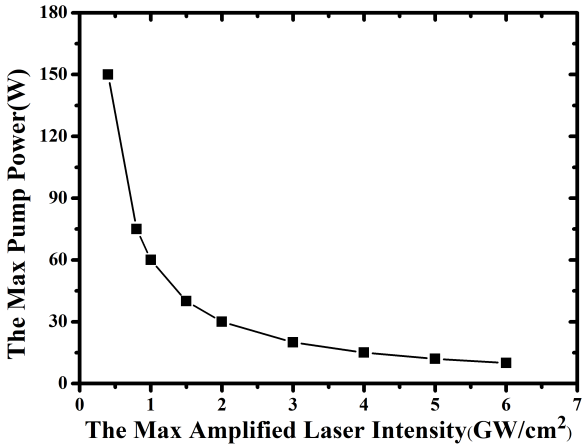

Figure 5. The relationship between the maximum pump power and the maximum laser intensity in an end-pumped Nd:YVO_4 amplifier at a QCW pump duty cycle of 10%.

In the main amplifier, the absorption efficiency of Nd:YVO_4 (0.2%, 1.5 cm) with absorption coefficient was 2.5 cm^{-1} and could reach 95%. Based on Equation (6), the calculated maximum average pump power was about 60 W at 1 kHz with QCW pump duty cycle of 10%, so each sub-amplifier pumped by 50 mJ pulses can work safely. Table 1 shows parameters of the picosecond amplification stages. With an input energy of 4.5 mJ and a total of 300 mJ pump energy into the main amplifier, we achieved maximum output energy of 65.4 mJ, corresponding to an optical efficiency of 20.3%. The spot size in different stages were gradually increased to ensure the laser intensity was below 1 GW/cm^2 and reduce the Raman gain. At different amplified stages, $I_{max} * L_{crystal}$ in each stage had the maximum value of 1.31 and below the SRS threshold of 1.55. In addition, catadioptric mirrors between the two amplifiers are anti-reflective coated to reduce the accumulation of Raman light. Via these measures, we achieved tens of mJ energy sub-ns pulse through a Nd:YVO_4 amplifier without the SRS process, as shown in Figure 6. There is no Raman light at a wavelength of 1176 nm (first Stokes wave) and wavelength 1313 nm (second Stokes wave) in the maximum laser output.

Table 1. Parameters of the sub-ns amplification stages.

Stage	E_{pump} [mJ]	E_{out} [mJ]	D_{out} [mm]	η_{o-o} [%]	I_{max} [GW/cm^2]	$L_{crystal}$ [cm]	$I_{max} * L_{crystal}$ [GW/cm]
Seed	-	0.055	-	-	-	-	-
Pre-amplifier	28.6	4.5	2.0	16.7	0.32	1.0	0.32
Main amplifier 1	100	22.8	2.6	18.3	0.72	1.5	1.08
Main amplifier 2	100	44.9	3.4	22.1	0.82	1.5	1.23
Main amplifier 3	100	65.4	4.0	20.5	0.87	1.5	1.31

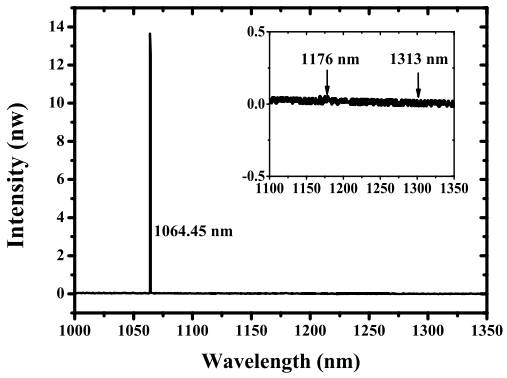

Figure 6. Obtained spectrum of the maximum laser output.

Figure 7 shows the spectra of the oscillator and amplifying systems. This sub-nanosecond oscillator had several longitudinal modea. The main longitudinal mode got more amplification, and, after pulse amplification, spectrum bandwidth became narrower. Narrower spectrum caused by gain narrowing would increase pulse width. A change of pulse width after amplification was shown in Figure 8. The pulse from the oscillator and amplifying systems was measured by a 8 GHz analog oscilloscope and an InGaAs photodiode (UPD-70-IR2-P, ALPHALAS). The pulse width of the oscillator is 450 ps. The pulse width of amplifying systems was 600 ps, corresponding to 109 MW pulse peak power.

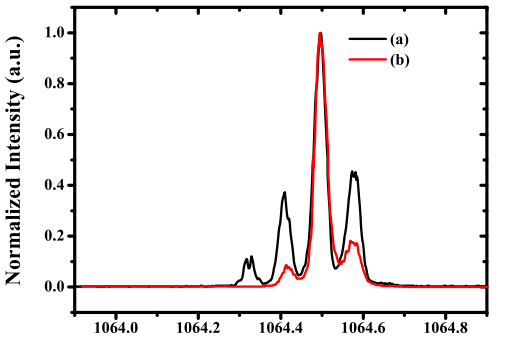

Figure 7. Pulse spectrum of: (**a**) the oscillator (**b**) via the amplifying system.

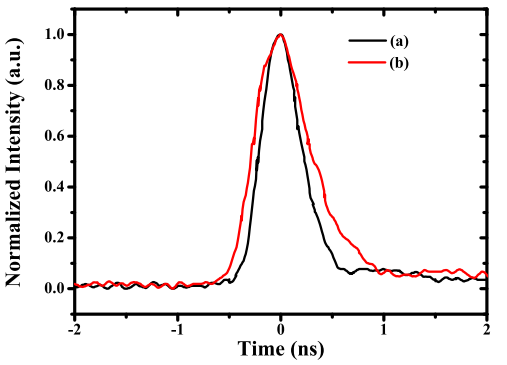

Figure 8. Pulse temporal width of: (**a**) the oscillator (**b**) via the amplifying system.

The beam images of this amplifying system are shown in Figure 9. The beam images were measured with a commercial CCD setting at a position which was about 1 m away from each amplifier.

The laser beam of pre-amplifier had good Gaussian distribution. With the increment of pulse energy in the main amplifier, beam center intensity gradually increased due to self-focusing, which could lead to little beam deterioration, as illustrated in Figure 10. The output beam of the oscillator was near diffraction limitation with $M_x^2 \times M_y^2 = 1.28 \times 1.20$. The M^2 for the horizontal and vertical axes via the amplifying system were 1.50 and 1.57, respectively. The results show the amplifier system still kept good beam quality using diode-end-pumped Nd:YVO_4 amplifier architecture when running at 1 kHz.

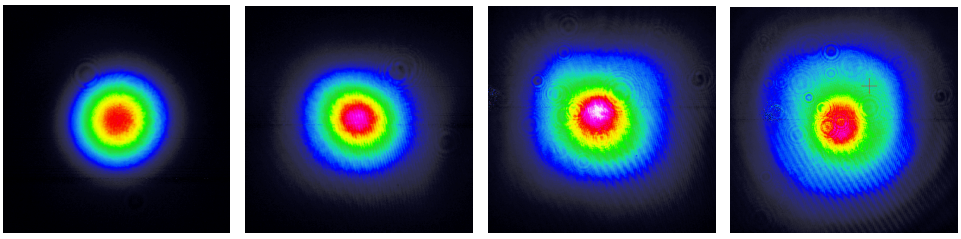

Figure 9. Beam images of each stage. (**a**) pre-amplifier; (**b**) stage 1 in main amplifier; (**c**) stage 2 in main amplifier; (**d**) stage 3 in main amplifier.

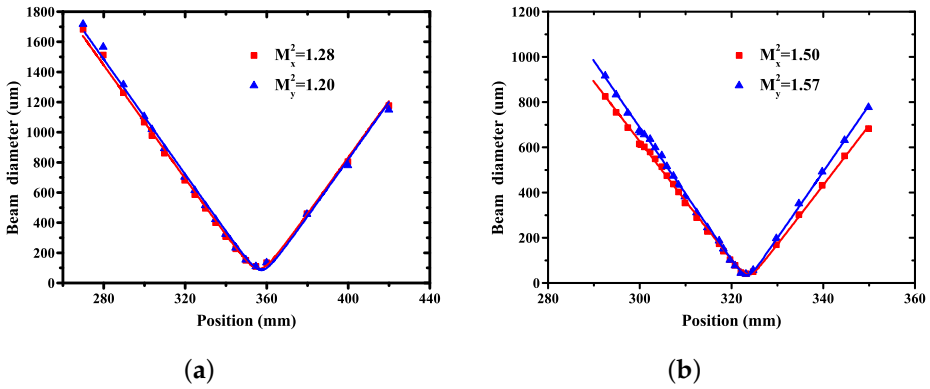

Figure 10. Beam quality factor M^2 of (**a**) the oscillator (**b**) via the amplifying system.

A 9 × 9 × 20 mm^3 type I LBO ($\theta = 90°$, $\phi = 10.8°$) crystal was used for extra-cavity frequency doubling. Maximum pulse 532 nm green light energy of 40.5 mJ was obtained at the maximum pump energy. The conversion efficiency was 61.8% and corresponding green light power was 40.5 W. The one-hour power stability has thus been tested, and 0.28% RMS was achieved, as shown in Figure 11. Figure 12 shows beam quality of green light were 1.26 and 1.25 for the horizontal and vertical axes. The beam distribution is also showed as the color image insets in Figure 12. The beam quality of green light was better than that of fundamental light, which is because the nonlinear process during frequency doubling can filter out the stray light with low peak power.

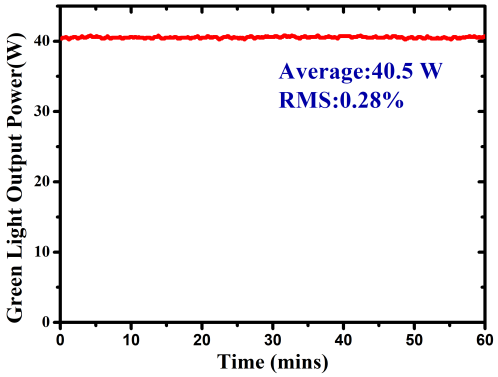

Figure 11. Energy stability of amplified pulses from the whole amplifier.

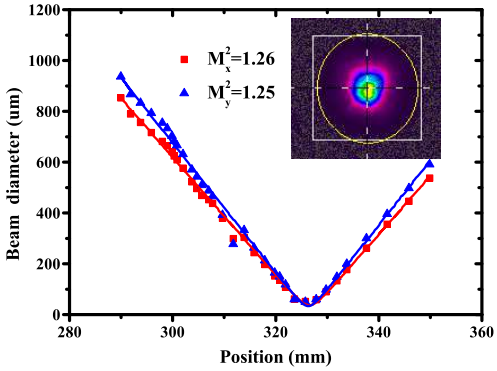

Figure 12. Beam quality factor M^2 of green light. The insets show the beam distribution of green light.

3.3. Conclusions

In conclusion, we have demonstrated a compact and efficient sub-nanosecond diode-end-pumped Nd:YVO_4 laser system. An off-axis four-pass diode-end-pumped Nd:YVO_4 amplification architecture was designed as a pre-amplifier. The main amplifier is composed of three stages, which include two single pass end-pumped Nd:YVO_4 sub-amplifiers. A maximum output energy of 65.4 mJ at 1 kHz without the stimulated Raman scattering (SRS) process was obtained with pulse duration of 600 ps, corresponding to 109 MW peak power. Good beam quality was obtained with $M^2 < 1.6$, and the excellent signal to noise ratio was more than 42 dB. Using LBO crystal, 40.5 W of 532 nm green light and a 0.28% power stability (RMS) were achieved. We also analyzed the influence of the SRS process on working parameters of diode-end-pumped bulk Nd:YVO_4 amplifier. At the high peak power amplifier, the limitation of diode-end-pumped pump power of bulk Nd:YVO_4 crystal due to suppression of the SRS process and thermal fracture. Our work offers an approach to estimate the maximum amplified ability of end-pumped Nd:YVO_4 crystal for high peak power laser amplification. This end-pumped Nd:YVO_4 sub-nanosecond laser system with high energy and good beam quality has simple and compact structure, which makes this laser an attractive light source for remote laser ranging.

Author Contributions: We confirm that all authors contributed substantially to the reported work. Y.H. was the main originator of this study and conceived most of the experiments; H.Z.; X.Y. performed the experiments and analyzed the data; Z.K. and F.L. participated in the research design and laser system adjustment; Z.F. supervised the project and provided the facilities. All the authors discussed and interpreted the results. All the authors read the final manuscript.

Acknowledgments: The work was supported by the project of National a thousand program from Academy of opto-electronics, Chinese academy of sciences (Y80B22A13Y) and the Development of High Power Nanosecond Laser Precision & Detecting Instrument Foundation (Grant No.ZDYZ2013-2).

Conflicts of Interest: The authors declare no conflict of interest.

Abbreviations

The following abbreviations are used in this manuscript:

MDPI	Multidisciplinary Digital Publishing Institute
DOAJ	Directory of open access journals
TLA	Three letter acronym
LD	linear dichroism

References

1. Ostermeyer, M.; Kappe, P.; Menzel, R.; Wulfmeyer, V. Diode-pumped Nd: YAG master oscillator power amplifier with high pulse energy, excellent beam quality, and frequency-stabilized master oscillator as a basis for a next-generation lidar system. *Appl. Opt.* **2005**, *44*, 582–590. [CrossRef] [PubMed]

2. Zhai, D.; Li, Y.; Xu, R.; Fu, H.; Zhang, H.; Li, Z.; Xiong, Y. Design and Realization of Single Telescope Transmitting and Twin Receiving Laser Ranging System at Yunnan Observatories. *Astron. Res. Technol.* **2017**, *14*, 310–316.
3. O'Neill, W.; Li, K. High-quality micromachining of silicon at 1064 nm using a high-brightness MOPA-based 20-W Yb fiber laser. *IEEE J. Sel. Top. Quantum Electron.* **2009**, *15*, 462–470. [CrossRef]
4. Deyra, L.; Martial, I.; Balembois, F.; Diderjean, J.; Georges, P. Megawatt peak power, 1 kHz, 266 nm sub nanosecond laser source based on single-crystal fiber amplifier. *Appl. Phys. B* **2013**, *111*, 573–576. [CrossRef]
5. Major, A.; Sukhoy, K.; Zhao, H.; Lima, I. Green sub-nanosecond microchip laser based on BiBO crystals. *Laser Phys.* **2011**, *21*, 57–60. [CrossRef]
6. Petrov, V.; Marchev, G.; Schunemann, P.G.; Tyazhev, A.; Zawilski, K.T.; Pollak, T.M. Sub-nanosecond, 1-kHz, temperature-tuned, non-critical mid-IR OPO based on CdSiP 2 crystal pumped at 1064 nm. In Proceedings of the Conference on Lasers and Electro-Optics, San Jose, CA, USA, 16–21 May 2010.
7. Chuchumishev, D.; Gaydardzhiev, A.; Fiebig, T.; Buchvarov, I. 0.7 mJ, 0.5 kHz Mid-IR Tunable PPSLT Based OPO Pumped at 1064 nm. In Proceedings of the Advanced Solid-State Photonics, San Diego, CA, USA, 29 January–1 February 2012.
8. Marchev, G.; Petrov, V.; Tyazhev, A.; Pasiskevicius, V.; Thilmann, N.; Laurell, F.; Buchvarov, I. Sub-nanosecond, 1-kHz, low-threshold, non-critical OPO based on periodically-poled KTP crystal pumped at 1064 nm. In *Nonlinear Frequency Generation and Conversion: Materials, Devices, and Applications XI*; International Society for Optics and Photonics: San Francisco, CA, USA, 15 February 2012; Volume 8240, p. 82400D.
9. Chuchumishev, D.; Gaydardzhiev, A.; Richter, C.; Buchvarov, I. 5 mJ, sub-nanosecond PPSLT OPA at 0.5 kHz, tunable in the water absorption band at 3 microns. In Proceedings of the IEEE 2013 Conferenceon and International Quantum Electronics Conference Lasers and Electro-Optics Europe (CLEO EUROPE/IQEC), Munich, Germany, 12–16 May 2013.
10. Chuchumishev, D.; Gaydardzhiev, A.; Fiebig, T.; Buchvarov, I. Subnanosecond, mid-IR, 0.5 kHz periodically poled stoichiometric LiTaO 3 optical parametric oscillator with over 1 W average power. *Opt. Lett.* **2013**, *38*, 3347–3349. [CrossRef]
11. Kyusho, Y.; Arai, M.; Mukaihara, K.; Yamane, T.; Hotta, K.; Kuwano, Y.; Saito, S. High-energy subnanosecond compact laser system with diode-pumped, Q-switched Nd: YVO_4 laser. In Proceedings of the Advanced Solid State Lasers, San Francisco, CA, USA, 31 January 1996.
12. Gaydardzhiev, A.; Trifonov, A.; Fiebig, T.; Buchvarov, I. High-power diode pumped Nd: YAG master oscillator power amplifier system. In *International Conference on Ultrafast and Nonlinear Optics 2009*; International Society for Optics and Photonics: Bourgas, Bulgaria, 2009; Volume 7501, p. 750105.
13. Yu, A.; Krainak, M.; Betin, A.; Hendry, D.; Hendry, B.; Sotelo, C. Highly Efficient Yb: YAG Master Oscillator Power Amplifier Laser Transmitter for Lidar Applications. In Proceedings of the Conference on Lasers and Electro-Optics 2012, San Jose, CA, USA, 6–11 May 2012.
14. Druon, F.; Balembois, F.; Georges, P.; Brun, A. High-repetition-rate 300-ps pulsed ultraviolet source with a passively Q-switched microchip laser and a multipass amplifier. *Opt. Lett.* **1999**, *24*, 499–501. [CrossRef]
15. Höiminger, C.; Zhang, G.; Moser, M.; Keller, U.; Johannsen, I.; Giesen, A. Diode-pumped thin disc Yb:YAG regenerative amplifier. In Proceedings of the Advanced Solid State Lasers, Coeur d'Alene, ID, USA, 2 February 1998.
16. Kaksis, E.; Andriukaitis, G.; Flöry, T.; Pugžlys, A.; Baltuška, A. 30-mJ 200-fs cw-Pumped Yb:CaF2 Regenerative Amplifier. In Proceedings of the Conference on Lasers and Electro-Optics, San Jose, CA, USA, 5–10 June 2016.
17. Agnesi, A.; Dallocchio, P.; Pirzio, F.; Reali, G. Sub-nanosecond single-frequency 10-kHz diode-pumped MOPA laser. *Appl. Phys. B* **2010**, *98*, 737–741. [CrossRef]
18. Jelínek, M.; Kubeček, V.; Čech, M.; Hiršl, P. 0.8 mJ quasi-continuously pumped sub-nanosecond highly doped Nd: YAG oscillator-amplifier laser system in bounce geometry. *Laser Phys. Lett.* **2011**, *8*, 205. [CrossRef]
19. Michailovas, K.; Smilgevičius, V.; Michailovas, A. High average power effective pump source at 1 kHz repetition rate for OPCPA system. *Lith. J. Phys.* **2014**, *54*. [CrossRef]
20. Liu, J.; Wang, W.; Wang, Z.; Lv, Z.; Zhang, Z.; Wei, Z. Diode-pumped high energy and high average power all-solid-state picosecond amplifier systems. *Appl. Sci.* **2015**, *5*, 1590–1602. [CrossRef]

21. Oreshkov, B.; Chuchumishev, D.; Iliev, H.; Trifonov, A.; Fiebig, T.; Richter, C.P.; Buchvarov, I. 52-mJ, kHz-Nd: YAG laser with diffraction limited output. In Proceedings of the IEEE 2014 Conference on Lasers and Electro-Optics (CLEO), San Jose, CA, USA, 8–13 June 2014; pp. 1–2.
22. Chuchumishev, D.; Gaydardzhiev, A.; Trifonov, A.; Buchvarov, I.C. 13-mJ, single frequency, sub-nanosecond Nd: YAG laser at kHz repetition rate with near diffraction limited beam quality. In Proceedings of the CLEO: Applications and Technology, San Jose, CA, USA, 6–11 May 2012.
23. Honig, J.; Halpin, J.; Browning, D.; Crane, J.; Hackel, R.; Henesian, M.; Peterson, J.; Ravizza, D.; Wennberg, T.; Rieger, H.; et al. Diode-pumped Nd: YAG laser with 38 W average power and user-selectable, flat-in-time subnanosecond pulses. *Appl. Opt.* **2007**, *46*, 3269–3275. [CrossRef] [PubMed]
24. Dong, J.; Liu, X.S.; Peng, C.; Liu, Y.Q.; Wang, Z.Y. High Power Diode-Side-Pumped Q-Switched Nd: YAG Solid-State Laser with a Thermoelectric Cooler. *Appl. Sci.* **2015**, *5*, 1837–1845. [CrossRef]
25. Bai, Z.A.; Fan, Z.W.; Bai, Z.X.; Lian, F.Q.; Kang, Z.J.; Lin, W.R. Optical fiber pumped high repetition rate and high power Nd: YVO_4 picosecond regenerative amplifier. *Appl. Sci.* **2015**, *5*, 359–366. [CrossRef]
26. Shen, Y.; Zhang, W.; Gong, M.; Meng, Y.; Wang, Y.; Fu, X. Four-Dimensional Thermal Analysis of 888 nm Pumped Nd: YVO_4 Dual-Rod Acousto-Optic Q-Switched Laser. *Appl. Sci.* **2017**, *7*, 470. [CrossRef]
27. Bai, Z.; Bai, Z.; Kang, Z.; Lian, F.; Lin, W.; Fan, Z. Non-Pulse-Leakage 100-kHz Level, High Beam Quality Industrial Grade Nd: YVO_4 Picosecond Amplifier. *Appl. Sci.* **2017**, *7*, 615. [CrossRef]
28. Li, R.; Bauer, R.; Lubeigt, W. Continuous-Wave Nd:YVO_4 self-Raman lasers operating at 1109 nm, 1158 nm and 1231 nm. *Opt. Express* **2013**, *21*, 17745–17750. [CrossRef]
29. Huang, G.; Yu, Y.; Xie, X.; Zhang, Y.; Du, C. Diode-pumped simultaneously Q-switched and mode-locked YVO_4/Nd: YVO 4/YVO_4 crystal self-Raman first-Stokes laser. *Opt. Express* **2013**, *21*, 19723–19731. [CrossRef]
30. Li, R.; Griffith, M.; Laycock, L.; Lubeigt, W. Controllable continuous-wave Nd:YVO_4 self-Raman lasers using intracavity adaptive optics. *Opt. Lett.* **2014**, *39*, 4762–4765. [CrossRef]
31. Kaminskii, A.A.; Ueda, K.i.; Eichler, H.J.; Kuwano, Y.; Kouta, H.; Bagaev, S.N.; Chyba, T.H.; Barnes, J.C.; Gad, G.M.; Murai, T.; et al. Tetragonal vanadates YVO_4 and $GdVO_4$–new efficient χ (3)-materials for Raman lasers. *Opt. Commun.* **2001**, *194*, 201–206. [CrossRef]
32. Zong, N.; Zhang, X.; Li, C.; Cui, D.; Xu, Z.; Zhang, H.; Wang, J. Stimulated Raman scattering of picosecond pulses in a YVO_4 crystal. *Laser Phys.* **2008**, *18*, 1544–1545. [CrossRef]
33. Chen, Y.F. Design criteria for concentration optimization in scaling diode end-pumped lasers to high powers: influence of thermal fracture. *IEEE J. Quantum Electron.* **1999**, *35*, 234–239. [CrossRef]
34. Bernhardi, E.; Forbes, A.; Bollig, C.; Esser, M.D. Estimation of thermal fracture limits in quasi-continuous-wave end-pumped lasers through a time-dependent analytical model. *Opt. Express* **2008**, *16*, 11115–11123. [CrossRef] [PubMed]